Supercritical fluid preparation of copper nanotubes and nanowires using mesoporous templates

2003 J. Phys.: Condens. Matter 15 8303

(http://iopscience.iop.org/0953-8984/15/49/009)

INSTITUTE OF PHYSICS PUBLISHING JOURNAL OF PHYSICS: CONDENSED MATTER

J. Phys.: Condens. Matter **15** (2003) 8303–8314 PII: S0953-8984(03)63513-7

Supercritical fluid preparation of copper nanotubes and nanowires using mesoporous templates

K J Ziegler, P A Harrington, K M Ryan, T Crowley, J D Holmes and M A Morris[1]

Dimensional Solids Group, Department of Chemistry, University College Cork, Cork, Republic of Ireland

E-mail: m.morris@ucc.ie

Received 14 May 2003, in final form 30 October 2003
Published 25 November 2003
Online at stacks.iop.org/JPhysCM/15/8303

Abstract

Supercritical fluid decomposition of copper precursors in the presence of hexagonal mesoporous silica matrices are used to prepare ordered copper metal nanowire and nanotube arrays. Evidence is presented which shows that the pore-filling process is accompanied by large expansions of the pore-to-pore distance induced by the inclusion process. Preparation of these materials requires strict control as copper appears to catalyze the collapse of the mesoporous structure. The copper nanostructures exhibit the normal face-centred cubic crystal structure although there is a strong variation of the lattice parameter with size. UV–visible absorption spectra of copper nanowires within the mesoporous matrix as a function of copper loading exhibit effects related to the low dimensionality of the nanowires formed. Transmission electron microscopy images and changes in the surface area and pore size of the materials as a function of copper content suggest that the growth mode is radial rather than a random nucleation and growth mechanism.

(Some figures in this article are in colour only in the electronic version)

1. Introduction

Strict control of dimension is required in the synthesis of nanostructures. This control not only ensures uniformity of the physical properties but also affords the opportunity to 'tailor' the performance of materials—specifically their electrical, magnetic, and optical properties. The requirement for dimensional control is particularly true of 1D (or more correctly high aspect ratio) structures, such as nanowires, because at small diameters quantum confinement can confer advantageous and tunable characteristics. However, preparation of nanowires at this scale (<10 nm) is difficult. The most important problem in these systems is the development of

[1] Author to whom any correspondence should be addressed.

0953-8984/03/498303+12$30.00

a method which can synthesize reasonable quantities of product whilst maintaining dimensional monodispersion. Further to these aims, it would be advantageous to prepare these wires in single crystal form and with preferred crystallographic orientations. Nanowire preparation has been reviewed [2, 3] and one promising technique of preparing quantum confined nanowires has been through the use of ordered mesoporous materials as templates in which material is deposited by supercritical fluid (SCF) decomposition of a suitable precursor [3–5]. Lyons *et al* [6] have shown that it is possible to alter the optical properties of silicon nanowires using size control of the mesoporous matrix. Very recently, it has been shown that this method can be adapted to allow the materials to be prepared as thin films in which the nanowires are single crystalline, and have specific crystal plane orientation and defined orientation to the film direction [7].

With this degree of control over the geometrical and structural arrangement it might be imagined that these systems may provide alternatives to lithography in the design of nanoelectronic circuitry. One of the key components in such design (and in nanodimensioned circuitry in general) would be the development of interconnects in the same dimensional range. One of the key aims of this work is to examine if our generic synthesis technique could be used to design electrically conducting metal nanowires within mesoporous frameworks. This synthesis offers some new challenges because of the requirement for strict chemical control (e.g. to avoid oxidation of the wires during preparation) together with the possibility of metal centres sponsoring mesoporous matrix decomposition.

2. Experimental details

The preparation of the mesoporous matrices used as templates is detailed elsewhere [3–6]. Briefly, P85 tri-block polyethylene oxide (PEO)–polypropylene oxide (PPO) surfactant ($PEO_{26}PPO_{39}PEP_{26}$) (Uniquema) was used as the organic template, tetramethoxysilane (TMOS) as the silicate source, and HCl as an acid catalyst. The solid obtained was calcined at 723 K for 24 h. The product is thought to be essentially 100% mesoporous based on pore volume measurements and extensive TEM studies. Powder x-ray diffraction (PXRD), transmission electron microscopy (TEM), and Brunauer Emmett Teller (BET) analysis (below) [8] suggest a pore-to-pore distance of 7.1 nm and a pore diameter of 5.5 nm. Samples (0.5 g) of mesoporous silica were degassed in N_2 at 473 K for 8 h prior to inclusion. Under glove box conditions (cleaned, dried nitrogen at positive pressures), the degassed material and copper precursor (at various concentrations) were placed in a 5 ml high-pressure reaction cell and sealed. Details of the SCF apparatus are presented elsewhere [2–7]. Here, CO_2 was used as the solvent and pressurized using an ISCO syringe pump (Lincoln, NE, USA). Prior to the reaction, the sample was flushed for several minutes with CO_2 to remove any air, etc. The cell was placed within a tube furnace and the pressure (207 or 345 bar) and temperature (400–800 K) ramped to the desired conditions and held constant for 30 min.

After the reaction, copper nanostructures could be isolated by dissolution of the silica matrix in a silox glass etch (ammonia fluoride solution) for 72 h. TEM analysis was carried out on a JEOL TEM-1200EX TEMSCAN instrument using an accelerating voltage of 80 kV. Typically, 20 mg of sample were dispersed by sonication in ethanol and a drop of the product placed on a carbon coated 400 mesh 3 mm diameter copper grid. The surface areas of the samples were measured using nitrogen BET isotherms at 77 K on a Micromeritics Gemini 2375 volumetric analyser. Each sample was degassed for 12 h at 573 K prior to measurement. The average pore size distribution of the calcined silicas was calculated using the Barrett–Joyner–Halanda (BJH) model [8] from a 50-point BET surface area plot. PXRD profiles were recorded on a Philips 3710 PWD diffractometer, equipped with a Cu Kα radiation source and standard

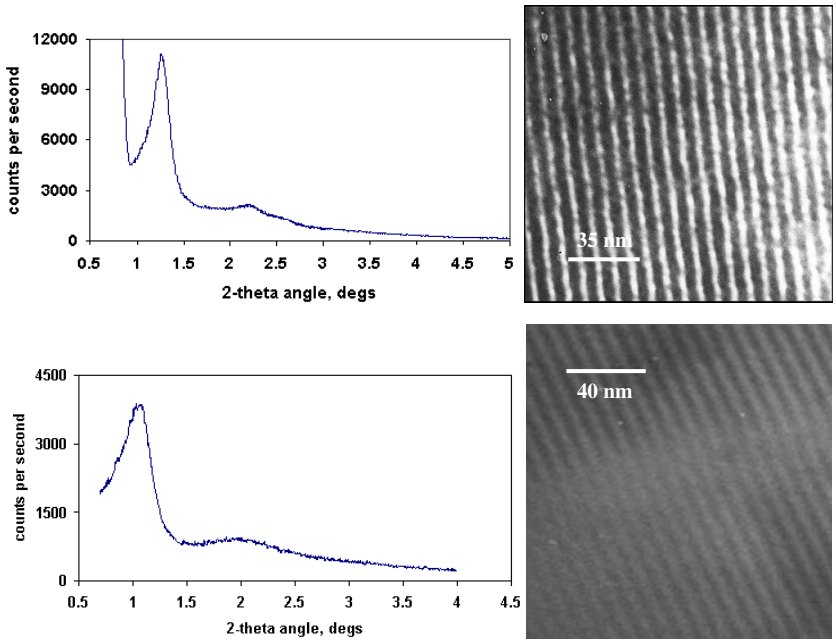

Figure 1. Comparison of PXRD profiles (left) and TEM images (right) from P85 derived mesoporous materials (upper) and after copper inclusion (1×10^{-3} mol of $Cu(HFAC)_2$) (lower).

Table 1. Summary of synthesis conditions for the preparation of copper nanowires within mesoporous matrices. ($Cu(HFAC)_2$ = copper (II) hexafluoroacetylacetonate dihydrate. $Cu(TFAC)_2$ = copper (II) trifluoroacetylacetonate. $Cu(ACET)_2$ = copper (II) acetate. $Cu(ACAC)_2$ = copper (II) acetylacetonate.)

Precursor	Temperature (K)	Pressure (bar)	Comments
$Cu(HFAC)_2.2H_2O$	473	207	Precursor did not completely decompose
$Cu(HFAC)_2.2H_2O$	573	207	Nanowires/tubes formed
$Cu(HFAC)_2.2H_2O$	773	345	Pore collapse, some CuO formation
$Cu(TFAC)_2$	773	345	Pore collapse
$Cu(TFAC)_2$	573	207	Pore collapse
$Cu(ACET)_2$	773	345	Pore restructuring
$Cu(ACAC)_2$	773	345	Pore restructuring

scintillation detector. Peak positions were estimated by Rietveld solution of the structure using PC Rietveld (Philips). UV–visible absorption spectra were collected on materials suspended in ethanol using a Hewlett-Packard 8453 diode array spectrophotometer.

3. Results

The products obtained were dependent on the copper precursor used and the pressure and temperature of the sc-CO_2 reaction cell. A summary of synthesis conditions for the precursors studied is provided in table 1. Great care was taken to carefully dry all solvents and maintain anhydrous conditions as trace amounts of water led to complete collapse of the mesoporous structure.

3.1. Mesoporous matrix formation

Evidence for pore filling (using $Cu(HFAC)_2$ precursor as described below) is witnessed in PXRD and TEM studies shown in figure 1. Before inclusion, the PXRD profile of the host matrix is typical of well-ordered mesoporous material with a (100) reflection at about 1.25° (2θ) and weaker (110) and (200) reflections at about 2.25° and 2.6°, respectively. These lattice spacings are consistent with a pore-to-pore distance of 7.02 nm. The BET surface area of the material was measured at 788.9 $m^2\ g^{-1}$ with a BJH [8] pore size of 5.53 nm. Using the hexagonal unit cell dimensions and the pore size, the total pore volume of the sample can be estimated at about 49% of total. The total pore volume as measured by BET isotherms gave slightly higher values (55%–65%) due to some microporous character, presumably within the pore walls. We do not believe that the methods used here are effective for pore filling of micropores and for this reason calculated pore volumes are used (see below). The measured surface area is consistent with this estimated porosity as the contribution of internal pore volume to the surface area would provide a surface area of about half this value. When the material was densified by air calcination at 1100 K for 24 h (this temperature was sufficient to produce low surface area materials without production of crystalline structure by PXRD), the density was measured at 2.77 g ml^{-1}. Using this density and the measured pore dimensions, the reaction weight of mesoporous silica (0.5 g) used in synthesis would require about 2.5×10^{-2} mol of copper to achieve complete pore filling. In practice, the amount required was much less than this value and this is discussed in greater detail below. The amounts of copper used in the experiments are given as mols of copper (in precursor form) added to the reaction cell and as a fraction of the amount required for complete pore filling. This latter measurement is described as δ, the fraction filling index (FFI).

3.2. $Cu(TFAC)_2$ precursor

The use of $Cu(TFAC)_2$ precursor led to the collapse of the pore structure. Temperatures above 573 K were required for precursor degradation and this always caused complete loss of pore structure and was readily observed in PXRD data where low-angle ($<5°\ 2\theta$) features were completely lost and large broad features appeared at about $22°\ 2\theta$ assigned to very poorly ordered silica (typical of data from dried and calcined TMOS). Diffraction features typical of face-centred cubic (FCC) copper were apparent at higher angles. Weak but sharp diffraction features on the leading edge of the broad feature could be observed around 17–18° 2θ. It is believed that this is the onset of crystallization of the material to quartz-like products.

3.3. $Cu(ACET)_2$ and $Cu(ACAC)_2$ precursors

These precursors also resulted in loss of the ordered pore structure but in a manner quite distinct from that observed in $Cu(TFAC)_2$. Precursor degradation led to the loss of all diffraction features arising from the hexagonally structured mesoporous silica. Unlike $Cu(TFAC)_2$, there is a only a very weak broad feature at about $22°\ 2\theta$ but of very low intensity. Intense and sharp diffraction features typical of FCC copper can be seen. The materials retain quite high surface areas ($>200\ m^2\ g^{-1}$) and worm-like pore structures were observed in TEM. Therefore, the data suggest that the mesoporous silica material has not crystallized or formed weakly ordered material as in the case for the $Cu(TFAC)_2$ derived materials. We believe these materials retain a disordered pore structure with amorphous silica walls. These materials can probably best be described as nanoporous. TEM micrographs of the copper component provide evidence for massive restructuring as seen in figure 2. Nanodimensioned copper wires and tubes can be clearly seen. However, there is a large spread in wire/tube width and the mean width is larger

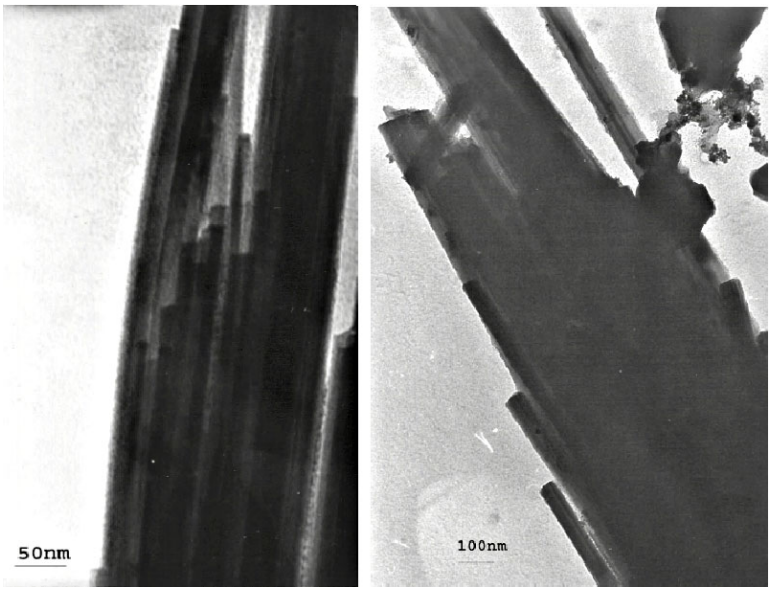

Figure 2. TEM images of two sets of nanowire bundles grown from SCF treatment of mesoporous matrix with $Cu(ACET)_2$ precursor (see table 1 and text). Scale as shown.

than the original pore size. It would seem likely that these wires have nucleated within the pores of the mesoporous structure which has collapsed during growth leaving the features to grow without constraint.

3.4. $Cu(HFAC)_2$ precursor

This precursor was the only one used that resulted in the growth of 1D copper structures that were constrained in diameter by the mesoporous matrix. Variations in experimental conditions suggested that the optimal decomposition temperature was 573 K. At lower temperatures, incomplete precursor decomposition was observed. At higher temperatures, PXRD data suggested pore collapse. There was also some evidence that copper oxide formed at these higher temperatures, indicating reaction with the mesoporous material or more likely the water present from the precursor.

The effects of treating the mesoporous P85 with 1×10^{-3} mol (FFI, $\delta = 0.077$) of copper precursor can be seen in figure 1. After precursor decomposition, the mesoporous structure is maintained, as witnessed by PXRD clearly indicating features assignable to a hexagonally structured lattice. However, the decomposition has caused the (100) reflection to decrease in intensity, broaden and move to lower angles (1.093° 2θ). Also, it is no longer possible to resolve shoulders between the (110) and (200) features. The overall area of the peak intensity has decreased by a factor of around 2.4 compared to that of the unreacted P85 derived silica. These data suggest that the mesoporous pore-to-pore distance has increased (from 7.02 to 8.09 nm), there is a loss of order (peak broadening), and that the total number of pores has decreased. The latter point is stressed: there is no dramatic change in pore size as shown by the BET data below; therefore, the decrease in peak intensity can only be ascribed to rearrangement of the mesoporous structure. The broadening of the diffraction peaks indicates that the pores are probably no longer completely parallel over their entire length. Evidence for expansion of

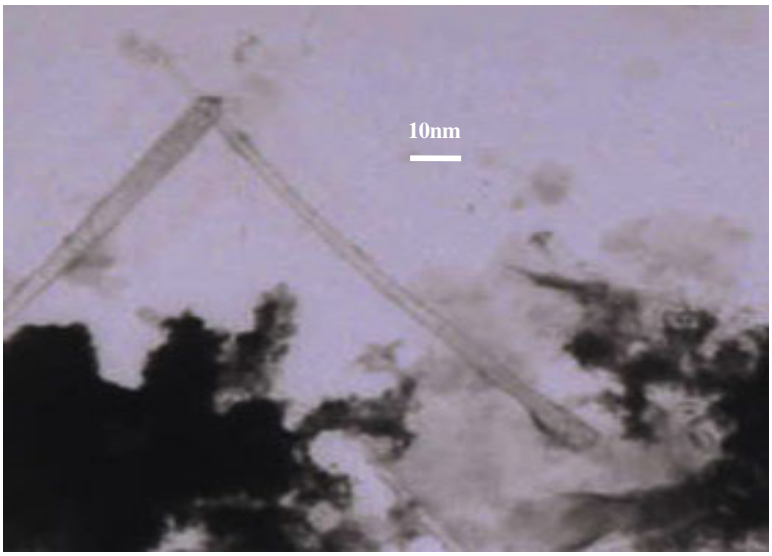

Figure 3. TEM images of copper nanotubes isolated after dissolution of the silica matrix. Three wires can be seen in the image shown.

the pore-to-pore distance is also provided in the TEM data in figure 1 which suggest about a 10% expansion of this parameter—consistent with the PXRD data.

The TEM data appear to indicate that the copper has been deposited within the pores as characterized by the change in contrast after inclusion. In addition, there is no evidence for particulate deposition as the pore images appear to be uniform in texture. Since less material is available than the amount required to fill the pores, the data would suggest that copper nanotubes are being formed in the material. All the TEM data collected as a function of copper loading suggested that all of the copper was deposited in this way and no evidence was seen for copper particle formation at the surface or within the pores at any time. More direct evidence for the formation of nanotubes is provided after the silica copper matrix was treated with the silox glass etch (figure 3). The nanotubes are not precisely uniform in width, and range from about 4 to 8 nm. It is believed that this is a result of the reduced ordering of the mesopore structure that results from the reaction.

The PXRD data discussed above showed a decrease in the area of mesoporous (100) peak by a factor of 2.4 compared to the original material. This reduction suggests that over 50% of the mesoporous structure has been lost, and this is also confirmed by the rapid decrease in surface area of the material once the precursor has been added (figure 4). In the initial reaction with 1×10^{-3} mol ($\delta = 0.077$) precursor the surface area decreases from 788.9 to 412.9 $m^2\ g^{-1}$. Higher amounts of precursor cause more gradual changes in surface area. Also shown in figure 6 is the corresponding decrease in the pore diameter, which can be easily used to estimate the loss of mesoporosity upon reaction. The pore diameter decreases progressively as the amount of copper increases. These changes, together with the TEM data presented above, would indicate that the nanowires/tubes grow radially from the pore wall inwards. It was not possible to collect meaningful pore size data at higher metal loadings than those described in figure 6. As can be seen in the plot in figure 6, the slope of the graph increases continually with loading as expected for radial growth. This is illustrated schematically in figure 7. For this growth mechanism, it can be written that the volume of copper added (V) is related to

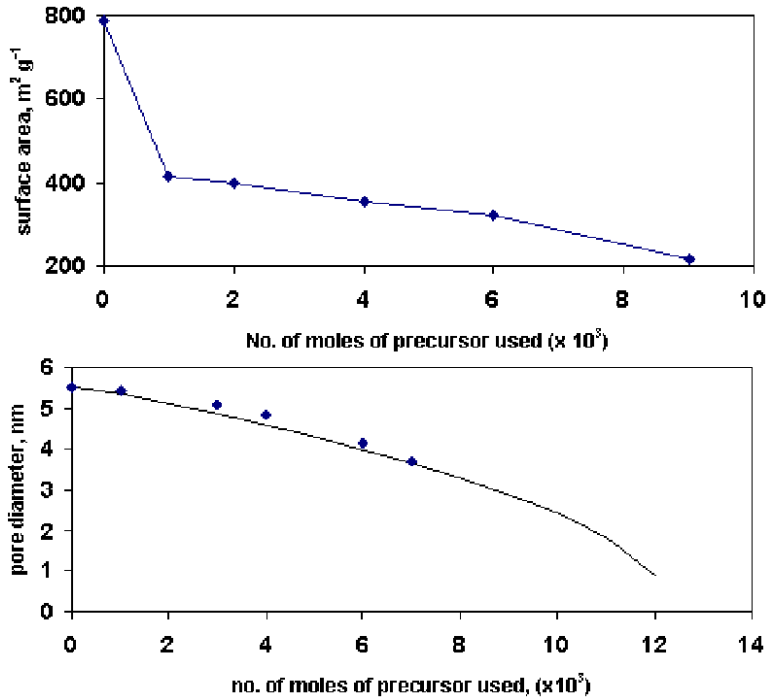

Figure 4. BET derived surface area (upper) and pore diameter (lower) as a function of the amount of precursor used. In the pore size data the solid curve is the theoretical fit to the data (see text).

the pore dimension decrease by $V = \pi l(r_0^2 - r_1^2)$, where l is the total length of all the pores and r_0 and r_1 are the radii of the unfilled and partially filled pore, respectively. The volume of copper is given directly from the amount of precursor and the known density of the FCC structure. A theoretical value of $V/\pi l$ of the original mesoporous material can be estimated at about 0.35 nm^2 using the unit cell, the pore-to-pore distance, and the pore size. In all cases, this value is close to that measured by BET derived total pore volumes; however, as stated above, this is believed to be less accurate because it contains microporous content which is not as well accessed and filled in these conditions. An experimentally measured value of $V/\pi l$ can be directly calculated by best-fitting of the data presented in figure 6 (as shown by the solid curve), and this gives a value of 0.63 nm^2. There is a large difference in the theoretical and actual values because the pore reordering results in a lower density of pores and lower total pore length compared to the unloaded material. The theoretical fit to the data points would indicate pore filling occurs at about 13×10^{-3} mol (i.e. an FFI value of 1 is assigned) of precursor. This would indicate that 50% of the pores have been lost.

3.5. Lattice parameter variation with copper nanotube wall thickness

High-angle PXRD data were collected from the copper nanowire/tube materials prepared from the Cu(HFAC)$_2$ precursor and are shown in figure 5. The copper x-ray reflection peak widths are narrow, with FWHM around 0.2° 2θ consistent with crystallite sizes of approximately 70 nm. Recent work by us on mesoporous silica-encapsulated germanium nanowires shows the wires to be single crystalline in nature [7]. We believe this is also the case here. Slight broadening of the reflections compared to large grain size solids is observed, but this is

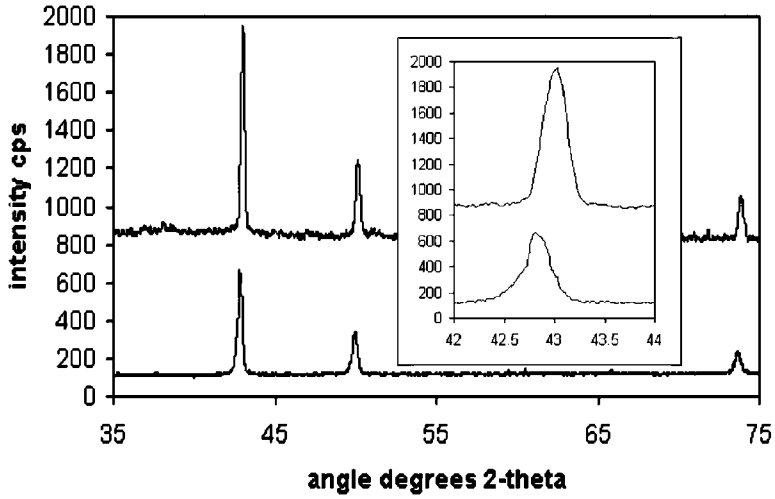

Figure 5. PXRD data of copper nanowires in the pores of mesoporous matrix as deposited by $Cu(HFAC)_2$. Two different loadings of 2 (lower) and 6×10^{-3} (upper) mols of copper were used. The inset is an expansion of the data from 42° to 44° 2θ to illustrate the shift in peak position and the unusual peak shape.

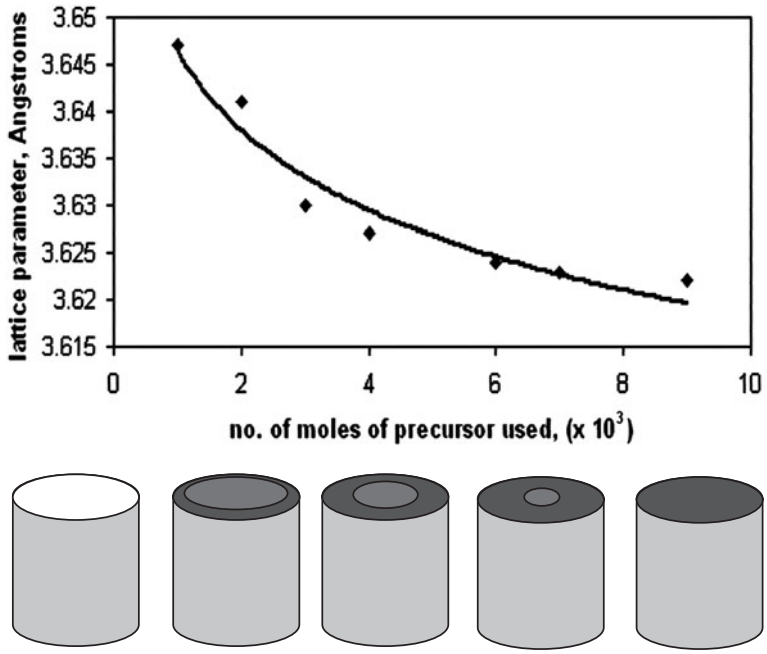

Figure 6. The lattice parameter of copper as a function of the amount of copper precursor used. The lattice parameter was estimated from the position of the (200) reflection at about 50° 2θ. A schematic diagram of the growth mode is shown below the data plot.

probably due to lattice strain (measured at about 0.3% from the PXRD data) in the constrained geometries. We have previously been able to observe two components of differing FWHM for the reflections observed from mesoporous constrained nanowires [5]. The narrow feature

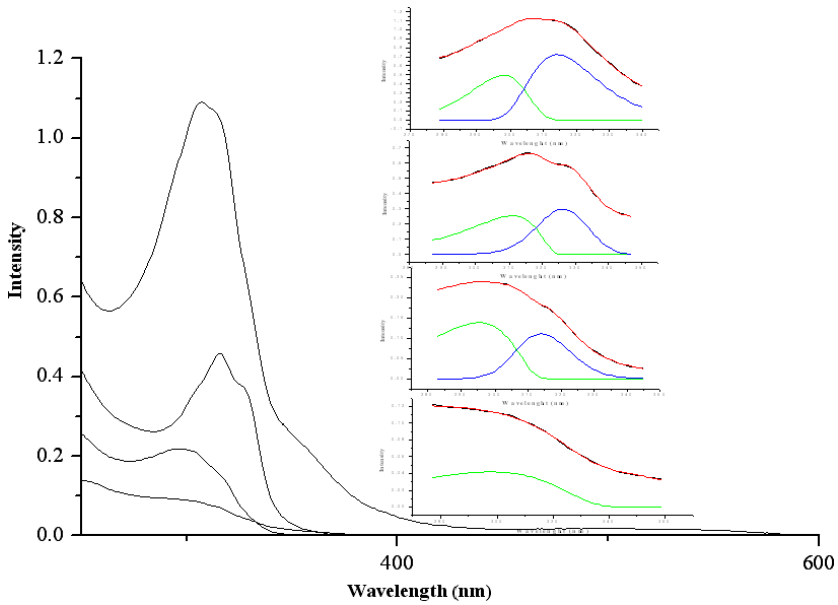

Figure 7. UV–visible absorption spectra of copper nanowires within the mesoporous matrix as a function of copper loading (1, 3, 5, 6×10^{-3} mols of precursor and intensity increases with loading as expected). Fits to the data are shown on the right (loading increases from bottom to top).

was assigned to reflections from planes along the wire length and the broader feature to planes across the nanowire. The copper nanowire PXRD can also be described in a similar fashion. The data displayed in figure 5 (for the low-loaded sample) exhibits strong broadening around the base of the reflection. This could not be adequately fitted with the normal pseudo-Voigt (mixed Gaussian–Lorenzian) shape normally used for fitting PXRD peaks and required a second component to be added to get adequate goodness of fit. However, detailed fitting was not possible here because it is thought that the wires are much longer than in the previous work and that the reflections from planes along the nanowire dominate the profile making peak-fitting of a low intensity feature in the base of the higher intensity feature unreliable.

What is striking about the PXRD data taken from the samples as a function of copper loading is an increase in peak position of the reflections with increasing amounts of copper, as shown in representative data in figure 5 (main and inset). These data suggest that the nanotubes exhibit a strong lattice parameter expansion from the value expected of bulk copper, 3.615 Å [10]. As the nanotube wall thickness increases as a function of copper loading, the lattice parameter tends to approach the bulk value. These data support the radial growth mode described above. One would not expect such a continual decrease in lattice parameter if growth was particulate in nature—particle sizes would remain approximately constant until higher FFI when coalescence of the particles occurred. It is clear that at over most of the loading range (at 7×10^{-3} mol or FFI = 0.54, the tube wall thickness is 0.93 nm) quantum confinement effects are important. As previously discussed by us contraction of the lattice parameter is more commonly observed [5]. However, these simple arguments do not account for some of the complex electronic changes that can take place in size-constrained particles [11].

Further evidence for the low dimensionality of the copper is provided by UV–visible absorption spectroscopy, as shown in figure 7. Nanoparticles of copper have been shown to exhibit two absorptions at around 300 and 500–600 nm [12]. The latter is more commonly

observed and can be assigned to plasmon resonances [13]. The peak at 300 nm has been theoretically predicted [14] and has been assigned to an interband transition [15]. For the materials prepared in this work, there is no indication of an absorption around 500–600 nm. This is consistent with suggestions that the 500–600 nm feature is not present for particle sizes less than 10 nm because of restricted electron mean free paths [16], and supports the argument that growth has been constrained within the pores of the mesoporous matrix. The interband transition is, however, intense and relatively sharp, suggesting some but not extensive distribution in particle sizes. As seen in figure 8, the intensity of the signal increases with increasing copper content. The spectra also seem to indicate that the peak is the result of the overlap of two component features. Fitting seems to suggest that the peak that is red-shifted increases in intensity with copper content, i.e. wall thickness. It is suggested that this is due to transverse modes across the cooper nanotube walls which grow in relative intensity as the walls increase in thickness, which is consistent with the evidence for radial growth modes presented above.

4. Discussion

It is, on first consideration, unexpected for growth of these wire/tubes to occur through quite a coherent radial growth mechanism. On careful consideration this is easily understood. Firstly, there is a thermodynamic driving force as radial growth decreases the surface area of the mesoporous material and hence the surface energy of the solid compared to less coherent growth schemes. Secondly, SCF conditions appear to favour single crystal growth (since mass transport rates can be higher than nucleation rates) [7]. Thirdly, SCF conditions offer little or no surface tension effects at the liquid solid interface, thereby minimizing kinetic requirements to rapid mass transport through the pore system, which favours uniform growth rather than unidirectional growth. These are key points. Recent data suggest that transport in mesopores at moderate to high pressure is dependent on the solvent and not the solute properties [17]. The relationship of the degree of pore filling to pressure has been well demonstrated [18] and more recently Do has shown that in SCF conditions, pore filling is achieved by a layer growth mechanism at high enough pressures [19].

The data indicate that even in the optimized system, significant amounts of pore reordering are observed. This pore collapse is in direct contrast to other systems prepared in these laboratories [3–7]. This contrast seems to be related to the ability of copper to sponsor devitrification of glass into crystalline phases[2]. Therefore, there is a need to investigate alternative precursors which will decompose at lower temperatures without destroying the pore structure of the mesoporous phase.

There is considerable controversy regarding the relationship between lattice dimensions and size for small particles. It is clear for compound materials, that as size reduces then lattice expansion occurs [11]. Such clarity is not possible for metal particles. This may be related to experimental problems. Broad size distributions and small particle sizes may hamper accurate x-ray determination of the lattice parameter. Further, adsorption may have an important role in determining lattice parameters [20]. However, the methods used here produce size-monodispersed particles with sufficient length to produce very narrow diffraction features, enabling very accurate determination of the lattice parameter from diffraction data. Containment in the mesoporous system will also limit adventitious chemisorption. Therefore, it is suggested that these data represent some of the most accurate measurements of the lattice parameter of dimension limited particles to date. Lattice contraction has been noted elsewhere

[2] http://www.geqonline.com/en/thermal.htm

for small copper systems but this work is now quite old [21] and surprisingly few sets of data have been reported. This is largely due to the accuracy in diffracted peak position required for lattice parameter determination and the experimental problems in obtaining such accuracy for small particles (as described above) Lattice contraction is often explained as resulting from compressive stresses developed from surface tension effects [5]. However, electronic effects may also be important. This can be due to charge transfer to a host matrix (e.g. Cu particles in carbon [22]) or e-transfer and charge screening effects at the particle surface. Electronic effects are likely to be dominant in this system. Strong surface core level shifts to lower binding energies have been observed for copper due to narrowing of the d band at the surface [23]. This would have a profound effect in these systems which contain high surface to volume ratios. Lowering of the copper d band electron binding energies can be interpreted as a weakening of the Cu–Cu bond and hence expansion of the bond length, consistent with the results presented here. The importance of electronic effects compared to simple stress arguments is clearly demonstrated by our UV-emission data. Detailed theoretical modelling of these systems is being carried out by us.

This method for the preparation of nanowires might have implications in the future design and fabrication of nanoelectronic circuitry and in particular to interconnect issues. The method specifies how uniformly sized metal nanowires may be prepared in bulk form with high yields. Further, these materials are highly crystalline and should exhibit much smaller electrical resistance to more polycrystalline materials. The preparation of tube-like entities might also be important in the design of nanotransitors since junctions could be formed by filling the core of the tube with a secondary material. Whilst this method is not yet perfected, it does point to how such heterosystems may be produced commercially.

Acknowledgments

The authors would like to thank Enterprise Ireland, the HEA (Ireland) PRTL and Intel (Ireland) for financial support. We would also like to thank the staff of the EMU at Cork for all their help. Professor Spalding is thanked for his advice on the choice of copper precursors.

References

[1] Serena P A and García N (ed) 1997 *Proc. NATO Advanced Research Workshop (Madrid, Spain, Sept. 1996)* (*NATO Science Series: E: Applied Sciences*) (Dordrecht: Kluwer–Academic)
[2] Niklasson G A 1999 *Nanostruct. Mater.* **12** 725
[3] Coleman N R, Morris M A, Spalding T R and Holmes J D 2001 *J. Am. Chem. Soc.* **123** 187–8
Coleman N R, O'Sullivan N, Ryan K M, Holmes J D, Spalding T R and Morris M A 2001 *J. Am. Chem. Soc.* **123** 7010
[4] Holmes J D, Spalding T R, Ryan K M, Lyons D, Crowley T A and Morris M A 2002 *Nanoporous Materials III* vol 141, ed A Sayari and M Jaroniec (Amsterdam: Elsevier) p 337
[5] Coleman N R, Holmes J D, Spalding T R and Morris M A 2001 *Chem. Phys. Lett.* **343** 1
[6] Lyons D M, Ryan K M, Morris M A and Holmes J D 2002 *Nano Lett.* **2** 811
[7] Ryan K M, Erts D, Olin H, Morris M A and Holmes J D 2003 *J. Am. Chem. Soc.* **125** 6284
[8] Barrett E P, Joyner L G and Halanda P P 1951 *J. Am. Chem. Soc.* **73** 373
[9] Ryan K M, Coleman N R B, Lyons D M, Morris M A, Steytler D C, Heenan R K and Holmes J D 2002 *Langmuir* **18** 4996
[10] Waldo G 1935 *Am. Mineral.* **20** 590
[11] Fukuhama M 2003 *Phys. Lett.* A **313** 427
[12] Lutz T, Estournès C, Merle J C and Guille J L 1997 *J. Alloys Compounds* **262** 438
[13] Cason P J, Miller M E, Thompson J B and Roberts C B 2001 *J. Phys. Chem.* B **105** 2297
[14] Trotter D M Jr, Schreurs J W H and Tick P A 1982 *J. Appl. Phys.* **53** 4657
[15] Ehrenreich H and Philipp H R 1962 *Phys. Rev.* **128** 1622

[16] Creighton J A E 1991 *J. Chem. Soc. Faraday Trans.* **87** 3881
[17] Clifford T 1998 *Fundamentals of Supercritical Fluids* 1st edn (New York: Oxford University Press)
[18] Benzinger W and Huttinger K S 1999 *Carbon* **37** 181
[19] Do D D and Do H D 2002 *AIChE J.* **48** 2213
[20] Kuhrt C and Anton R 1991 *Thin Solid Films* **198** 301
[21] Wasserman H J and Vermaak J S 1970 *Surf. Sci.* **22** 164
[22] Popescu R, Macovei P, Devory A, Manaika R, Barna P B, Kovacs A and La'Ba'n J L 2000 *Eur. Phys. J.* B **13** 737
[23] Webber P R and Morris M A 1984 *Phys. Rev.* B **29** 5957